Optimal Design of a State Feedback Sliding Mode Controller of a Loaded Double Inverted Pendulum

Manar Lashin[a], Ahmed Ramadan[b]

[a]*Mechatronics and Robotics Eng. Dept., Egypt-Japan University of Science and Technology, E-JUST- Alexandria, Egypt*
[b]*Computers and Automatic Control Dept., Tanta University, Tanta, Egypt*

Abstract

In this article, the stabilization problem of a loaded double inverted pendulum using an optimized state feedback sliding mode controller is investigated. ADAMS/Matlab co-simulation environment is used for building a virtual nonlinear model for a loaded double inverted pendulum system and a state feedback sliding mode control law is designed for stabilizing the system. The proposed procedures introduce a methodology for designing an optimized state feedback sliding mode controller for unperturbed and perturbed systems. Moreover, the invariance condition is discussed followed by controller design for matched and mismatched uncertainties. Genetic Algorithms are used to optimize the parameters of the sliding mode controller based on a performance index containing the sum of squared errors. The proposed control scheme can significantly suppress chattering effect and improves the performance of the system against uncertainties. Simulation results show the effectiveness of the approach and the robustness of the system against payload changes.

Keywords: Sliding Mode Controller, Optimization, Matched/Mismatched uncertainties, Invariance Condition, Loaded Double Inverted Pendulum, Co-Simulation, ADAMS/MATLAB co-simulation.

1. Introduction

Inverted pendulum (IP) system is a benchmark control problem for stability and robustness studies. It is a naturally unstable and under-actuated system. The control of IP is challenging; it can be divided into three aspects, swing-up (1; 2), stabilization (3; 4) and tracking control problems (5). On the other hand, controlling a double inverted pendulum (DIP) is more challenging than the common inverted pendulum as increasing the number of links does increase the complexity and uncertainty of the system. Stabilization of a loaded double inverted pendulum (LDIP) is the scope of this work. Several Stabilization control problems can be simplified as an inverted pendulum stabilization problem. For instance, to maintain a Humanoid (6; 7) in an upright posture under large disturbance, to keep a space shuttle balanced during launching, and stabilization of a segway vehicle during its motion (8; 9).

A stabilization fuzzy control based on fusion function has been presented in (10) for stabilizing a DIP. Simulation results showed that the proposed scheme can stabilize the system in a relatively short time. However, the approach did not consider the robustness issue in the design. A comparative study between LQR and Adaptive-Neuro Fuzzy inference system (ANFIS) has been proposed in (11). The ANFIS based controller succeeded to stabilize the system for a wide range of initial conditions in comparison with the LQR one. However, the performance of both controllers did not provide satisfactory results in terms of settling time, overshoots and control effort. A hierarchical sliding mode controller for a DIP system has been introduced in (12). A sliding mode controller (SMC) has been designed and stability analysis has been investigated at certain initial states without considering uncertainties. A sophisticated self-tuning Neuro-PID controller was proposed in (13), which kept the angular positions of its links at small values. However a hunting motion was observed on the cart.

In general, the SMC law provides an effective and robust way of controlling nonlinear systems. It has a good dynamic performance with uncertainties, if the controlled system satisfies the invariance condition. Therefor, the system behavior is independent of the uncertainties and disturbances. This identical to one of two major problems in designing SMC:

1. ensuring the existence of matching condition.
2. ensuring no chattering behavior.

The first condition guarantees the controller robustness while the second condition suppresses the chattering assists in protecting the mechanical components such as actuators from damage due to the high frequency components and prevents exciting non-modeled dynamics. To verify the presented approaches, ADAMS (Automatic Dynamic Analysis of Mechanical Systems) is employed. The design tool provided by ADAMS used to build a virtual LDIP model. The main contribution of this work is the augmentation between optimization search techniques (GAs) with a well-known approaches in designing state feedback SMC for stabilizing LDIP. These approaches are: Ackermann and Utkin for controlling unperturbed system and perturbed system with matched uncertainties (14; 15) and Shyu method for controlling the perturbed system with mismatched uncertainties (16). The validity of both control techniques is proofed via ADAMS/Matlab co-simulation environment. The presented control methodologies deals with the invariance condition and eliminates the chattering effect.

This paper organized as follow: Section II briefly introduces the system mathematical model. In Section III, the sliding mode controller is presented for unperturbed/perturbed systems and the invariance condition is discussed. The optimization of sliding mode controller parameters based on GAs are explained in Section IV. In Section V, simulation results based on ADAMS/Matlab co-simulation are presented and analyzed. Finally, Section VI draws the conclusion.

2. Mathematical model

The LDIP system is graphically shown in Fig.1. The model of LDIP consists of a cart which moves horizontally, two arms with uniform mass distribution over the whole arm length and a payload which has a significant inertia, that is attached to the second link. The mathematical model can be obtained according to the principles of dynamics and kinematics. The derivation of the equations of dynamic model is carried out using Euler Lagrange equation. This results in the nonlinear representation of the system (17).

$$\frac{d}{dt}\frac{\partial L}{\partial \dot{x}} - \frac{\partial L}{\partial x} + \frac{\partial P}{\partial x} + \frac{\partial S}{\partial \dot{x}} = F \tag{1}$$

where, L is the Kinetic energy, P is the potential energy, S is the energy losses. x represent the variables of the generalized coordinates (z, θ, ϕ). While F is a vector of forces or moments acting in the direction of the generalized coordinates. After calculations of the terms

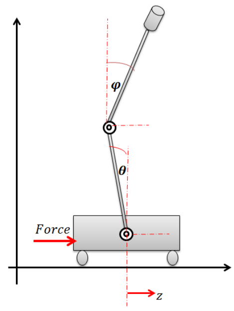

Figure 1: Schematic configuration of a loaded double inverted pendulum

of kinetic and potential energy of the system parts, energy losses and the forces applied to the system, equation (1) is built. The dynamics of the considered system are given as:

$$d_1\ddot{z} + d_4(\cos\theta)\ddot{\theta} + d_5(\cos\phi)\ddot{\phi} + c_1\dot{z} - d_4(\sin\theta)\dot{\theta}^2 - d_5(\sin\phi)\dot{\phi}^2 = f \tag{2}$$

$$d_4(\cos\theta)\ddot{z} + d_2\ddot{\theta} + d_6(\cos(\theta-\phi))\ddot{\phi} + d_6(\sin(\theta-\phi))\dot{\phi}^2 - d_4 g(\sin\theta) = 0 \tag{3}$$

$$d_5(\cos\phi)\ddot{z} + d_6(\cos(\theta-\phi))\ddot{\theta} + d_3\ddot{\phi} - d_6(\sin(\theta-\phi))\dot{\theta}^2 - d_5 g(\sin\phi) = 0 \tag{4}$$

The nonlinear representation of the system can be rewritten into a much more compact form:

$$N(q)\ddot{q} + H(q,\dot{q})\dot{q} + g(q) = F \tag{5}$$

where, $N(q)$ is the inertia tensor:

$$N(q) = \begin{pmatrix} d_1 & d_4(\cos\theta) & d_5(\cos\phi) \\ d_4(\cos\theta) & d_2 & d_6(\cos(\theta-\phi)) \\ d_5(\cos\phi) & d_6(\cos(\theta-\phi)) & d_3 \end{pmatrix},$$

and, $\ddot{q}$ is the acceleration vector $[\ddot{z} \quad \ddot{\theta} \quad \ddot{\phi}]$,

$H(q,\dot{q})$ is the Coriolis matrix :

$$H(q,\dot{q}) = \begin{pmatrix} c_1 & -d_4(\sin\theta)\dot{\theta} & -d_5(\sin\phi)\dot{\phi} \\ 0 & 0 & d_6(\sin(\theta-\phi))\dot{\phi} \\ 0 & -d_6(\sin(\theta-\phi))\dot{\theta} & 0 \end{pmatrix},$$

and, g includes gravity terms:

$$g = [0 \quad -d_4 g\sin\theta \quad -d_5 g\sin\phi)]^T,$$

where, F the vector of forces:

$$F = [f \quad 0 \quad 0]^T,$$

The values of $d_1, d_2, \cdots, d_6$ are given as follows:
$d_1 = M + m_1 + m_2 + m_3$

$d_2 = J_1 + m_1 l_1^2 + m_2 L^2 + m_3 L^2$
$d_3 = J_2 + m_2 l_2^2 + J3 + m_3 L_0^2$
$d_4 = m_1 l_1 + m_2 L + m_3 L$
$d_5 = m_2 l_2 + m_3 L_0$
$d_6 = m_2 L l_2 + m_3 L L_0$

The state variables are given by:

$$\dot{x} = [z, \theta, \phi, \dot{z}, \dot{\theta}, \dot{\phi}]^T,$$

where, $z, \dot{z}$ are the cart position and velocity respectively $\theta, \dot{\theta}$ are first link angular position and angular velocity respectively and $\phi, \dot{\phi}$ are the second link angular position and angular velocity respectively. The description of the system parameters are given in Table.1(11). The nonlinear model equations are linearized at the equilibrium point $z, \theta, \phi \approx 0, 0, 0$. This linearization results in:

Table 1: Double Inverted Pendulum Model Parameters

Symbol	Description
m_1	Mass of the first link assembly ($0.205kg$)
m_2	Mass of the second link assembly ($0.178kg$)
m_3	Mass of the payload ($0.432kg$)
M	Mass of the cart assembly ($1.67kg$)
l_1	Length from the first joint to the center of mass of the first link ($0.180m$)
l_2	Length from the second joint to the center of mass of the second link ($0.185m$)
L	length of the first link ($0.36m$)
L_0	length of the second link($0.37m$)
J_1	Mass moment of inertia of the first link around its center of gravity($0.0041kg.m^2$)
J_2	Mass moment of inertia of the second link around its center of gravity ($0.0024kg.m^2$)
J_3	Mass moment of inertia of the payload around its center of gravity ($0.00014kg.m^2$)
c_1	Friction coefficient between the cart and the linear guide ($0.21N.sec/m$)

$$\dot{x} = Ax + Bu, \quad y = Cx + Du, \tag{6}$$

$$A = \begin{pmatrix} 0 & 0 & 0 & 1 & 0 & 0 \\ 0 & 0 & 0 & 0 & 1 & 0 \\ 0 & 0 & 0 & 0 & 0 & 1 \\ 0 & 4.5381 & -0.4210 & -0.117 & 0 & 0 \\ 0 & 149.6361 & -105.6702 & -0.3643 & 0 & 0 \\ 0 & -140.605 & 135.1784 & 0.0450 & 0 & 0 \end{pmatrix},$$

$$B = \begin{pmatrix} 0 \\ 0 \\ 0 \\ 0.5174 \\ 1.7706 \\ -0.18546 \end{pmatrix}, C = \begin{pmatrix} 1 & 0 & 0 & 0 & 0 & 0 \\ 0 & 1 & 0 & 0 & 0 & 0 \\ 0 & 0 & 1 & 0 & 0 & 0 \end{pmatrix},$$

$$D = \begin{pmatrix} 0 \\ 0 \\ 0 \end{pmatrix}.$$

However, ADAMS facilitates obtaining both the linear and nonlinear model directly from the graphical representation.

3. Sliding Mode Controller

3.1. State Feedback SMC: An overview

The design of SMC includes two parts:
1) selection of the plane in which the sliding motion is stable $S = C^T x = 0$ (C^T is an n-dimensional constant row vector. A proper choice of this vector, determines the dynamic properties of the sliding plane). then,
2) designing the control law which enforces the sliding mode in this sliding plane.
The sliding mode equation is of $(n-1)th$ order and does not rely on disturbance. If the invariance condition is satisfied. The traditional method in designing sliding mode controller is to derive the sliding function first and thereafter, by conventional methods of the linear theory the sliding control can be driven. The sliding mode control law basically consist of two parts:

$$u(t) = u_c(t) + u_{eq}(t), \qquad u(t) \in \mathbb{R}^m \tag{7}$$

where $u_c(t)$ is the corrective control used to compensate the deviations from the sliding plane. $u_{eq}(t)$ is the equivalent control or the robust control which guarantees that the derivatives of the sliding plane are equal to zero to stay on the sliding surface. It can be obtained from a conventional method of the linear system theory. The conventional methods in the design of SMC is to convert the system into the well-known canonical form. The SMC canonical form consist of two blocks:

$$\dot{x_1} = A_{11}x_1 + A_{12}x_2 \tag{8}$$

$$\dot{x_2} = A_{21}x_1 + A_{22}x_2 + B_2 u \tag{9}$$

where, $x_1 \in \mathbb{R}^{n-m}$, $x_2 \in \mathbb{R}^m$ and $det(B_2) \neq 0$. The nonsingular coordinate transformation:

$$\begin{bmatrix} x \\ y \end{bmatrix} = Tx \quad , T = \begin{bmatrix} I_{n-m} & -B_1 B_2^{-1} \\ 0 & B_2^{-1} \end{bmatrix} \tag{10}$$

where,

$$B = \begin{bmatrix} \mathrm{B}_1 \\ \mathrm{B}_2 \end{bmatrix}$$

A_{ij} are constant matrices for i, j=1, 2. If the pairs (A, B) is controllable the pairs (A_{11}, A_{12}) is also controllable. The $(n - m)$ desired eigenvalues may be assigned by a proper choice of the vector C^T (for single input system $m = 1$).

$$x_2 = C^T x_1, \tag{11}$$

Sliding mode should be enforced in the manifold:

$$S = x_2 + C^T x_1 = 0 \tag{12}$$

Robustness of SMC which make the system insensitive to disturbances requires the invariance condition to be satisfied. The invariance condition defined by (18) as: a disturbance can be rejected by a control law if and only if the control subspace spans the disturbance subspace. A discontinuous control action can force the system to move along the sliding surface such that its behavior is only determined by the sliding surface parameters and not influenced by uncertainties or disturbance. This is the so-called completely robust feature of SMC, for which it is assumed that the uncertainties and disturbance satisfy the matching condition. The disturbance affecting the system motion in general whether matched or mismatched are:
(a) the disturbance up to the beginning of the sliding mode. This kind determines the initial conditions of the sliding mode, and
(b) the disturbance after the sliding mode begins.
The trajectory of the sliding mode motion will depend only on the value of disturbance up to the beginning of the sliding mode via the initial conditions. The precursory part of the motion is abbreviated if the control function properly chosen. Which means that the whole system exhibits a low sensitivity to disturbance.

3.2. State Feedback SMC for Unperturbed Systems

Unlike the traditional method in designing SMC, Ackermann and Utkin introduce a method to determine the sliding plane parameters in an explicit form without need to transform the system to the canonical form of SMC. Similarly as a linear state-feedback scalar control law can be found explicitly resulting in a system with desired eigenvalues via Ackermann's formula. This approach valid only if the invariance condition is satisfied $D \in span(B)$. The vector C^T may be found in an explicit form without the sliding motion equation.
For an arbitrary system:

$$\dot{x} = Ax + Bu \tag{13}$$

$$u = -k^T x, \quad k^T = e^T P(A) \tag{14}$$

$$e^T = [0 \cdots 01][b \quad Ab \cdots A^{n-1} b]^{-1} \tag{15}$$

$$C^T = e^T P_1(\lambda) \tag{16}$$

with,

$$\begin{aligned} P_1(\lambda) &= (\lambda - \lambda_1)(\lambda - \lambda_2) \cdots (\lambda - \lambda_{n-1}) \\ &= P_1 + P_2 \lambda + \cdots + P_{n-1} \lambda^{n-2} + \lambda^{n-1} \end{aligned} \tag{17}$$

The real or pairwise conjugate complex value $\lambda_1, \lambda_2, \cdots, \lambda_{n-1}$ are the desired eigenvalues of the sliding mode dynamics on the plane $S = C^T x = 0$. Where λ_n can take any arbitrary value. In (19), λ_n is the remaining pole, is used to provide some stability margin for the system by accelerating the reaching phase. The sliding mode can be enforced in an unperturbed system by:

$$u = -(\psi \|x\| + \delta) sign(S) \tag{18}$$

where, ψ is a finite positive value and δ an arbitrary positive value. The control tends to zero in the system with asymptotically stable sliding modes. The design procedures according to (14) is as follow:
1) the desired spectrum of the sliding motion λ_1, λ_2,$\cdots \lambda_{n-1}$ is chosen.
2) the equation of the discontinuity plane $S = C^T x = 0$ is found to be:

$$C^T = e^T (A - \lambda_1 I)(A - \lambda_2 I) \cdots (A - \lambda_{n-1} I) \tag{19}$$

Now, state feedback SMC can be designed according to (18).

3.3. State Feedback SMC for perturbed system

3.3.1. Matched Uncertainties

An arbitrary perturbed system can be designed by:

$$\dot{x} = Ax + B(u + f(t)) \tag{20}$$

where, $f(t)$ is the disturbance forces assuming that $|f(t)| \leq f_0 = Const$ and f_0 is assumed to be known. The control law is:

$$u = -M_0 sign(s), \quad M_0 = Const. \tag{21}$$

The discontinuous control u is designed to enforce sliding mode in the sliding plane $s = 0$. The values of S and $\dot{S}$ should have different signs in some vicinity of the plane. Due to the high switching function the system not reach the plane ideally but shows undesired chattering behavior. Which occurred if the control take only the two extremes values $+M_0$ or $-M_0$. Several methods were reported to reduce chattering. Some proposed modification in the discontinuous control law that instead of forcing the states to remain on the sliding plane $S = 0$, it will be allowed to remain within small boundary layer around the plane. This is done by replacing the *sign* function with *sat* function. In (20), adaptive fuzzy dead-zone is introduced as another solution to solve the problem of *sign* function discontinuity. The matched uncertainties will be represented by a Sin-wave with amplitude = 0.5 and frequency = $20[rad/sec]$. The control law according to (21) is designed for perturbed system with matched uncertainties.

3.3.2. Mismatched Uncertainties

For the perturbed model of LDIP the state space representation is represented as:

$$\dot{x} = Ax(t) + Bu(t) + f(x,t), \quad y = Cx + Du, \tag{22}$$

where, $f(x,t)$ is the disturbances. It is considered that the disturbances $f(x,t)$ is uniformly bounded with respect to time t, and locally is uniformly bounded with respect to state x.

$$f(x,t) = \triangle Ax(t) + f(t) \tag{23}$$

where, $\triangle A$ is the change in the state matrix A caused by maximum payload variation. For this case the maximum allowable payload is 5.6 times the mass of the second link or 2.30 times the nominal payload. While $f(t)$ is the matched disturbances and can be eliminated. The inherent feature of SMC is to overcome this disturbances. However, the main target is to optimized SMC law to overcome the mismatched type of disturbances. For the system in (2), The mismatched uncertainties represented by $f(x,t)$ cause the system to violate the invariance condition. Designing a sliding mode controller for such class of systems which dissatisfy this condition has been widely discussed. Some approaches require additional constraints before introducing a control law for such systems (21; 22). While in (23) the chattering effect may not included as an important issue in the design. In this paper the continuous control law proposed by (16) is used in designing state feedback SMC. In this control law the stability of the sliding plane and chattering elimination are considered important issues in the design. It guarantees asymptotic stability even if the system has mismatched uncertainties. For LDIP model the invariance condition is violated by payload variations. Moreover, the uncertainties of most real systems are not satisfying this assumption (24). Shyu (16) solve this problem by introducing a continuous state feedback sliding mode control law for the case of the mismatched uncertainties. This control law considers two main assumptions (Theorem 1):

1. There exists a known non-negative continuous. function $\rho(.)$ such that $\| f(x,t) \| \leq \rho(x,t)$ where $\| . \|$ denotes the standard Euclidean norm.

2. The pair (A, B) is controllable and the matrix B has full rank.

The continuous control law which drives the state trajectories of this system onto the sliding surface '$S(t) = 0$', and the system remains on it thereafter can be described as:

$$u(t) = -(CB)^{-1}[CAx(t) + PS(t)] - \bar{\rho}(x,t)\frac{\mu(x,t)}{\| S^T(t)CB \| (\| \mu(x,t) \| + \varepsilon e^{\alpha t})} \tag{24}$$

where, $P \in R^{m\times m}$, is a positive definite symmetric matrix, $\varepsilon, \alpha > 0$,

$$\bar{\rho}(x,t) = \| S^T(t)CB \| \rho(x,t) \tag{25}$$

$$\mu(x,t) = \frac{S^T(t)CB\rho(x,t)}{\| S^T(t)CB \|} \tag{26}$$

The state trajectories will hit the sliding surface $S = C^T x(t) = 0$ subject to any initial condition. Therefore, the system remains on the sliding plane as $t \to \infty$. Further details about theorem (1) proof can be found in (16). The maximum allowable value for the payload is 5.6 times the mass of the second link. The disturbance can be written as $\| f(x,t) \| \leq 169.9415x(t)$. In the control law (24), the sliding plane is asymptotically stable even the invariance condition is not satisfied. Which means that the plane is insensitive with respect to the disturbance. This conclusion lights up the method introduced by Ackermann and Utkin to obtain the vector C^T in an explicit form without the sliding motion equation using Ackermann's formula. Then the control law (24) can be designed with a proper choice of controller parameters P, ε and α.

4. Genetic Algorithms (GAs) Optimization

Like biological evolution, GAs as an optimization technique are used in solving the constrained and unconstrained optimization problems. The GAs start with a population of solutions that is modified through crossover and mutation operators. The algorithm randomly selects individuals from the current population which represents parents and generate the next generation; the children. This process is repeated for consecutive generations, till the population converges to an optimal solution with respect to the objective function chosen. For instance in LDIP model, the sum of the squared errors between the desired system response and the actual response is chosen as the objective function. Hence the optimization problem is a minimization of the objective function. Individuals with higher fitness values will have bigger chances for recombination and consequently for generating offspring (25). GAs have five major parameters to be determined (26):

1. Population size, which influences amount of search points/solutions in every generation
2. Crossover probability, which influences the efficiency of exchanging information. In general, the crossover probability is chosen between 0.6 and 1
3. Mutation probability, which occurs with a very small probability. The mutation probability is usually chosen as 0.01 or less. This value controlling the probability of production and crossover
4. Chromosome length, which influences the resolution of the searching result
5. Maximum number of generations, which influences the searching time and searching result. GAs with larger search space and less population size need more generations to reach a global optimum .

The standard architecture of GAs illustrated in Fig.2.

For the Control law (18),(21) and (24) there are six parameters that should be tuned in order to stabilize the LDIP system with reasonable control effort. These parameters are: ψ,δ,M,P, ε and α. GAs as an intelligent search technique sounds to be useful in defining their optimal values in terms of an objective function. The number of generations chosen is 100 with population size of 5 individuals and 2 sub-population. Increasing the number of generations or sub-populations over this value is found not to add any improvement in this optimization problem. However, these numbers have a remarkable effect in improving the optimization quality in general. The chosen objective function is the sum of squared errors for the cart position and the two link angles such that:

$$F = 1000 * (\Sigma {e_z}^2 + \Sigma {e_\theta}^2 + \Sigma {e_\phi}^2) \qquad (27)$$

The factor 1000 is a weighting factor to make the optimization process much more sensitive to small values of error. The optimization process is carried out based on ADAMS/Matlab co-simulation model.

5. Simulation Results

5.1. ADAMS Dynamic Modeling Software

Adams/Controls help in eliminating the need to write complex equations of motion describing mechanical plants or complex models. ADAMS provides graphical representation for modeling mechanical systems, containing a variety of constraints and force types as well as parts of arbitrary shape. ADAMS enables visualizing the results using animations and plotting that save time and money specially in complex models. ADAMS enables exporting 3-D mechanical systems from other specialized softwares such Solidworks and Catia in order to study alternative designs as ”virtual prototypes” by simulating and comparing realistic motion behavior. ADAMS is found to be useful for modeling the LDIP system as it is not a complex mechanical model that needs to be built in a specialized 3-D mechanical design software.

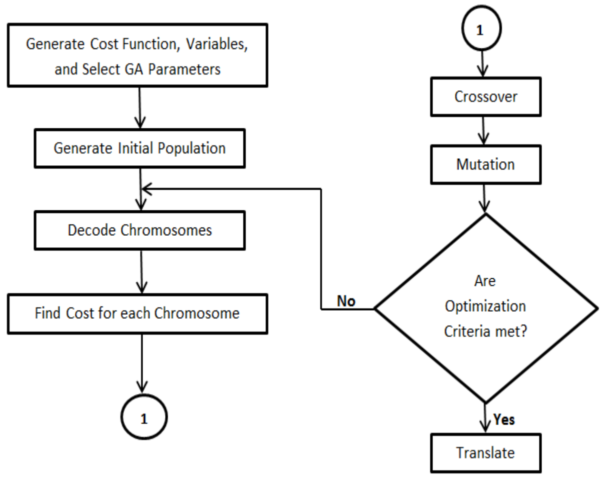

Figure 2: The standard architecture of Genetic Algorithms

Matlab provides an effective tool for controlling different systems. Co-simulation between these two softwares facilitate building a virtual environment for validating different control schemes. This environment is built by activating the control modules ’Adamas/Controls’ from the ’plug-in manager’ in ADAMS. The input force in ADAMS is supplied from MATLAB as a variable depending on the control architecture and the dynamic model of the system. ADAMS Input/Output variables are z, $\dot{z}$, θ, $\dot{\theta}$, ϕ, $\dot{\phi}$ as outputs while F, the control effort is the input. The co-Simulation sequence between ADAMS and MATLAB is:

- Build the mechanical model for the LDIP in ADAMS
- Define the measurements: z,θ, ϕ, $\dot{z}$,$\dot{\theta}$, $\dot{\phi}$
- Define the input force F as Matlab variable
- Choose form the Plug-in manger ”Adams/Control”

- Determine the Input/output variables for ADAMS
- Export the model to Matlab
- Apply the control scheme in the co-simulation environment

The parameters of the loaded double inverted pendulum found in table.I. The implementation of state feedback sliding mode control implies that all components of a state vector have to be accessible for measurement. However, this is not the case for many practical situations. To solve this problem a state observer to restore the state vector using available measurements of some states can be used. Some other techniques derive a class of systems such that the control task can be solved by designing an output feedback controller (27; 28; 14). In ADAMS all states can be measured directly and then exported to Matlab.

Co-simulation creates a feasible environment as a real-time experiment. Which assist in relying the results and provides higher fidelity of the proposed optimized control scheme. Moreover, co-simulation made it easier for modeling and debugging systems in comparison with traditional design strategy of mathematical methods. The linearized model of the double inverted pendulum is used in designing the SMC while the validation of the optimized SMC is applied on the nonlinear model established on ADAMS software.

5.2. Controller Design

To obtain the eigenvalues, LQR technique used to get the optimal closed loop poles:

$$v = \int_0^\infty (x^T Qx + u^T Ru)dt \tag{28}$$

where Q and R are the weighting matrices which are selected based upon the desired level of performance and permissible control energy levels. The chosen values for Q and R are: $Q = diag(7200, 36, 900, 252, 18, 36)$ $\quad R = 5.5$

The obtained closed loop eigenvalues for LDIP system are:

$\lambda_1 = -17.9326$ $\quad \lambda_2 = -14.5416$
$\lambda_3 = -2.8461 + 1.6541i$ $\quad \lambda_4 = -2.8461 - 1.6541i$
$\lambda_5 = -5.3130$

The optimized parameters of the sliding mode controller after optimization are $M = 92.7968$, $\psi = 0.3815$, $\delta = 231.9672$, $P = 2.39347$, $\varepsilon = 2.2943 \times (10)^{10}$ and $\alpha = 0.06969$. The parameters of the optimized state feedback sliding mode controller

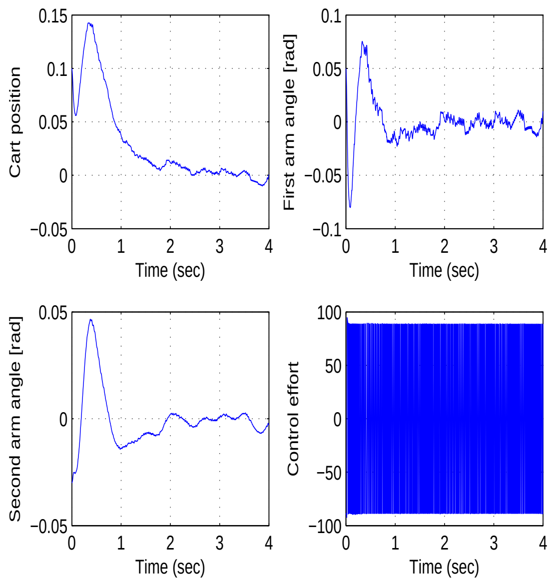

Figure 3: OSMC for unperturbed system using the discontinuous function '*sign*'; The cart position[m], first and second angles[rad] and control effort at initial states $z = 0.1m$, $\theta = 0.05rad$, $\phi = -0.03rad$

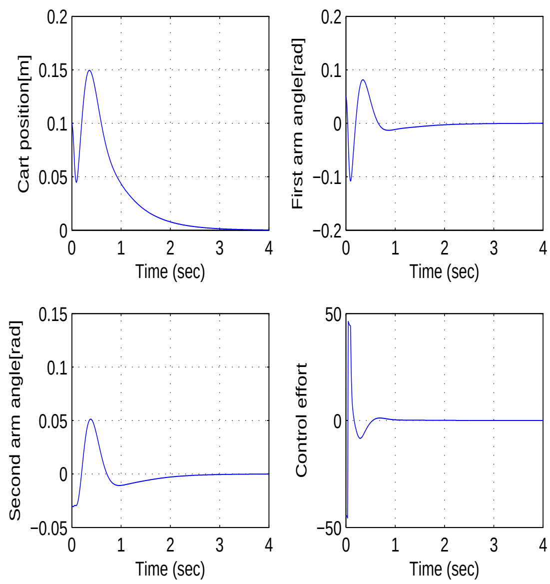

Figure 7: OSMC for unperturbed system: Cart position[m], first and second angles[rad] and control effort at initial states $z = 0.1m$, $\theta = 0.05rad$, $\phi = -0.03rad$

in the three cases assumed to be constant and not vary when the payload is changed. This is just to verify

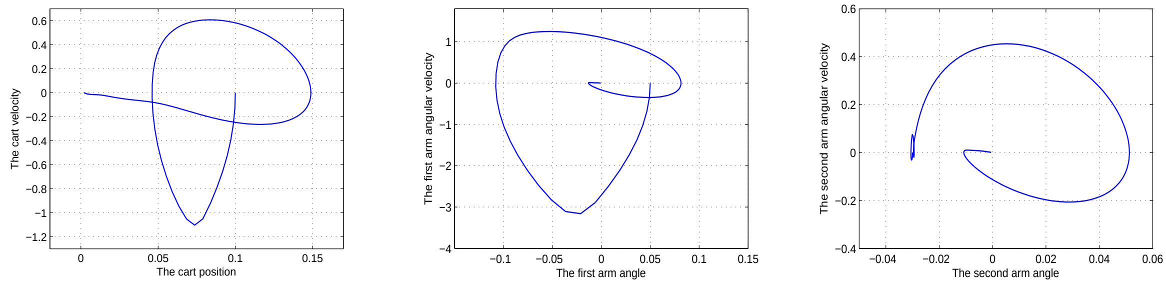

Figure 4: Phase trajectory between each two states in unperturbed DIP

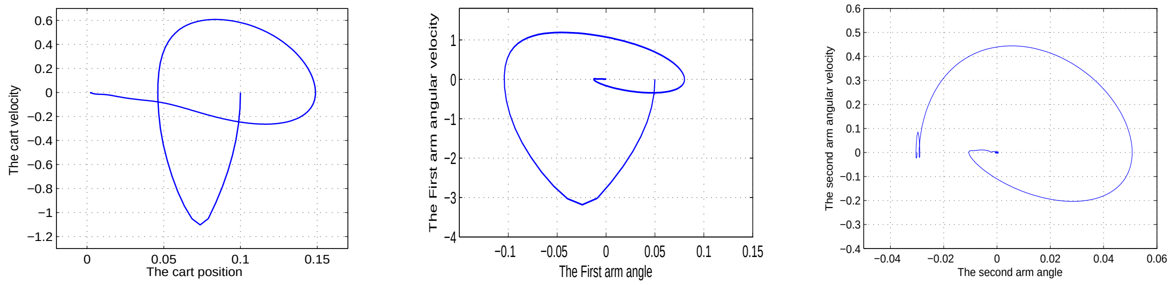

Figure 5: Phase trajectory between each two states in perturbed DIP with matched uncertainties

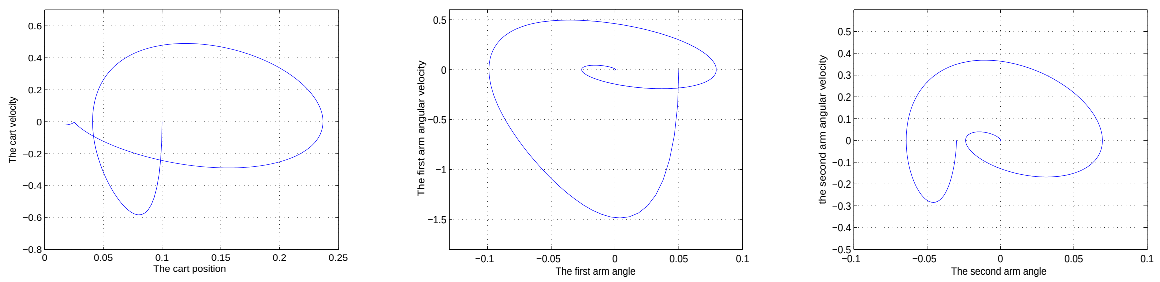

Figure 6: Phase trajectory between each two states in perturbed DIP with mismatched uncertainties

the robustness of the controller. In addition, the initial states of the cart movement and the links' angles are kept constant at values $z_{int} = 0.1m$, $\theta_{int} = 0.05rad$ and $\phi_{int} = -0.03rad$ with the load changes. For the control laws (18) and (21), the *sign* function cause chattering behavior to appear. Figure.3 show the chattering effect which raise due to forcing the system to be in the plane $S = 0$. Replacing *sign* with *sat* eliminate this problem.

Before investigating system performance under SMC we shall discuss an important issue, stability of the system under SMC for perturbed and unperturbed systems, matched and under mismatched uncertainties. Asymptotic stability means that the equilibrium is stable, and that in addition, states starts close to 0 actually converge to 0 as time $t \longrightarrow \infty$.

Definition: an equilibrium point 0 is asymptotically stable, and if it is stable, and if in addition there exist some r>0 such that $||x(0)||$<r implies that $x(t) \longrightarrow 0$ as $t \longrightarrow \infty$ (29). Figures.4, 5 and 6 shows that the in the three cases, the system can converge asymptotically to zero in a finite time. In OSMC for the unperturbed system, the maximum overshoots % and settling time *sec* are listed in table.2. Figure.7 show the Cart position[m], first and second angles[rad] and control effort at initial

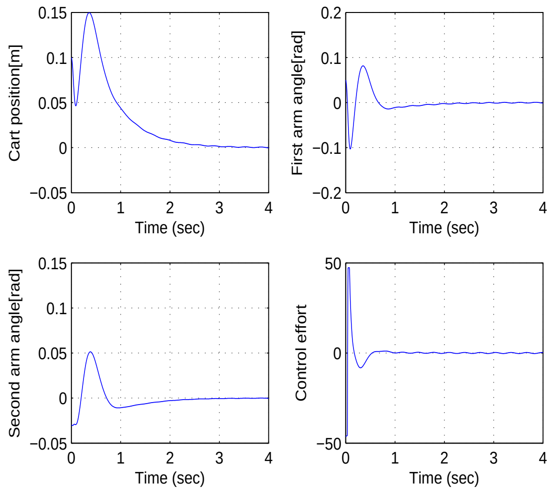

(a)

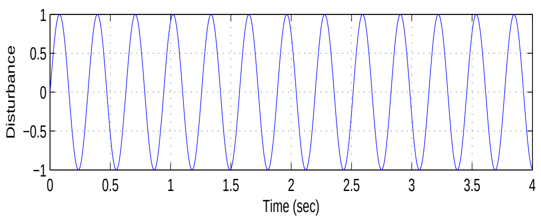

(b)

Figure 8: OSMC for perturbed system with matched uncertainties (a) the Cart position[m], first and second angles[rad] and control effort at initial states $z = 0.1m$, $\theta = 0.05rad$, $\phi = -0.03rad$ (b) Sin-wave disturbance of $Amp = 1$ and $frequency = 20[rad/sec]$

states $z = 0.1m$, $\theta = 0.05rad$, $\phi = -0.03rad$. In the case of perturbed system with matched uncertainties, the maximum overshoots % and settling time sec are listed in table.3. Figure.8 show the Cart position[m], first and second angles[rad] and control effort at initial states $z = 0.1m$, $\theta = 0.05rad$, $\phi = -0.03rad$. The

Table 2: Overshoots and settling time for unperturbed system

overshoots%			Settling Time(t_{ss})		
$z\%$	$\theta\%$	$\phi\%$	$t_{ss}(z)sec$	$t_{ss}(\theta)sec$	$t_{ss}(\phi)sec$
14.9%	10.7%	5%	$3.3sec$	$2.8sec$	$2.5sec$

LDIP model subjected to a sin-wave disturbance of $Amp = 0.5$ and $frequency = 20[rad/sec]$. When the states reach the sliding plane, the disturbance had no effect. Satisfying the invariance condition guarantees that the controller's behavior is only determined by the sliding surface parameters and not influenced by uncertainties or disturbance.

At different payloads, the controller show robustness

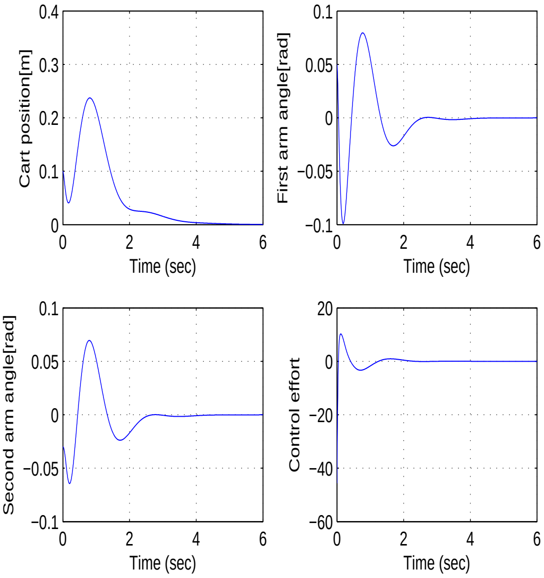

Figure 9: OSMC for perturbed system with mismatched uncertainties: Cart position[m], first and second angles[rad] and control effort at initial states $z = 0.1m$, $\theta = 0.05rad$, $\phi = -0.03rad$

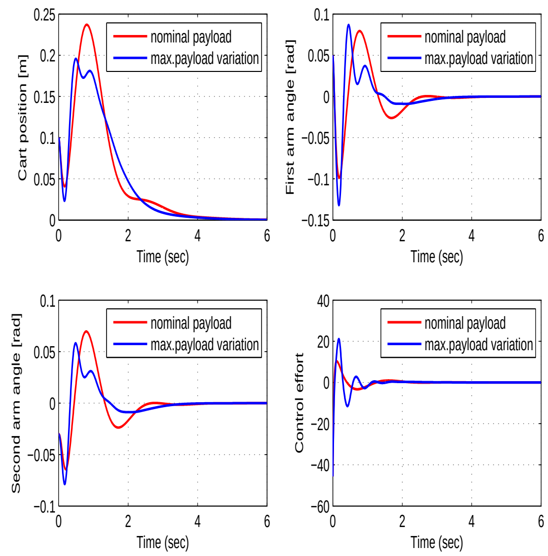

Figure 10: OSMC for perturbed system with mismatched uncertainties at the nominal payload and at the maximum payload variation: Cart position[m], first and second angles[rad] and control effort at initial states $z = 0.1m$, $\theta = 0.05rad$, $\phi = -0.03rad$,

and maintains the stability. Based on the design of optimized SMC for perturbed system with mismatched uncertainties presented in Section.3.3.2. The controller

Table 3: Overshoots and settling time for perturbed system with matched uncertainties

overshoots%			Settling Time(t_{ss})		
$z\%$	$\theta\%$	$\phi\%$	$t_{ss}(z)sec$	$t_{ss}(\theta)sec$	$t_{ss}(\phi)sec$
14.9%	10.3%	5%	$3sec$	$2.1sec$	$3sec$

Table 4: Overshoots and settling time for perturbed system with mismatched uncertainties

overshoots%			Settling Time(t_{ss})		
$z\%$	$\theta\%$	$\phi\%$	$t_{ss}(z)sec$	$t_{ss}(\theta)sec$	$t_{ss}(\phi)sec$
14.9%	10.7%	5%	$3.3sec$	$2.8sec$	$2.5sec$

still showing a robustness against payload variation in spite, the applied payload variation is 2.30 times the nominal payload. The maximum allowable payload is $0.9975kg$ and the mass moment of inertia is $0.00014kg.m^2$. In the case of perturbed system with mismatched uncertainties the maximum overshoots % and settling time *sec* are listed in table.4. In the three cases, the control effort is less than $\pm 47N$. Figures.9 and 10 show the output responses and the control effort for the perturbed LDIP in the case of nominal payload and at maximum payload variation in comparison with nominal payload respectively. By investigating the sliding surface Fig.11 in the case of OSMC for perturbed system with mismatched uncertainties we found that the optimized controller suppress chattering effectively. It seems from results that the OSMC which presented for unperturbed system and perturbed system with matched and mismatched uncertainties is effectively removes chattering with small control effort as possible. In addition, using GAs confers optimality to the algorithm as well guaranteeing minimum squared error.

5.3. Optimization Process Repetition

In the optimization process, the initial values for the parameters of the controller are set arbitrary. The optimized parameters can be used as the initial values for more optimization process. Therefor, the repetition of the optimization process has been discussed. In this stage, the repetition over five optimization process has been studied. In each process, the optimized values obtained for the parameters from the previous process are used as the initial values for the next one.

The output of this process is a data set for each parameter. This values are listed in the table.5. To further describe these data sets, measures of spread or dispersion are employed. One of the most commonly used measures is standard deviation. This value gives information on how the values of the data set are varying or deviating from the mean value. As some values are less than the mean, negative deviations will result, and for values greater than the mean positive deviations will be obtained. By simply adding the values of the deviations from the mean, the positive and negative values will cancel to result in a value of zero. By squaring each of the deviations, the problem of positive and negative values is avoided. There are two common definitions for the standard deviation s of a data vector X.

Table 5: Double Inverted Pendulum Model Parameters

The parameter	1^{st}	2^{nd}	3^{th}	4^{th}	5^{th}
ψ	0.3815	0.3399	0.3339	0.38147	0.350
δ	231.9672	230.39	234.86	231.418	234.01
M	92.7968	93.494	93.221	91.0495	92.0627
P	2.39347	2.814724	2.5915	2.2598	2.857667
ε	$2.2943 * 10^9$	$1.315226 * 10^9$	$2.031 * 10^9$	$2.81579 * 10^9$	$1.36341 * 10^9$
α	0.06964	0.063115	0.05224	0.066797	0.066184

The first form:

$$s = \sqrt{\frac{1}{n-1}\sum_{i=1}^{n}(x_i - \overline{x})^2} \tag{29}$$

The second form:

$$s = \sqrt{\frac{1}{n}\sum_{i=1}^{n}(x_i - \overline{x})^2} \tag{30}$$

where,

$$\overline{x} = \frac{1}{n}\sum_{i=1}^{n} x_i \tag{31}$$

where n is the number of elements in the sample. The two forms of the equation differ only in $n1$ versus n in the divisor. The value of the standard deviation for the parameters ψ, δ, M, P, ε and α are listed in table.6 Repeating the optimization process improves the overall performance of the controller in the two case: unperturbed SMC and for the perturbed system with mismatched uncertainties. Further tries were done to reduce the value of P. However, this value has a considerable effect in stabilizing the LDIP in the case of mismatched uncertainties. Figures 13, 12 and 14 shows the effect of repeating the optimization process. The perturbed system with matched uncertainties seems to to be improved by repeating the optimization process.

Table 6: Double Inverted Pendulum Model Parameters

The parameter	**Standard deviation**
ψ	0.0228
δ	1.8542
M	0.9859
P	0.2596
ε	6.365410^8
α	0.0068

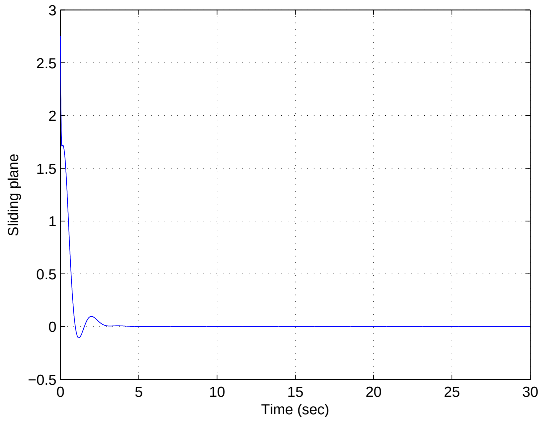

Figure 11: Sliding plane for OSMC for perturbed system with mismatched uncertainties at initial states $z = 0.1m$, $\theta = 0.05rad$, $\phi = -0.03rad$

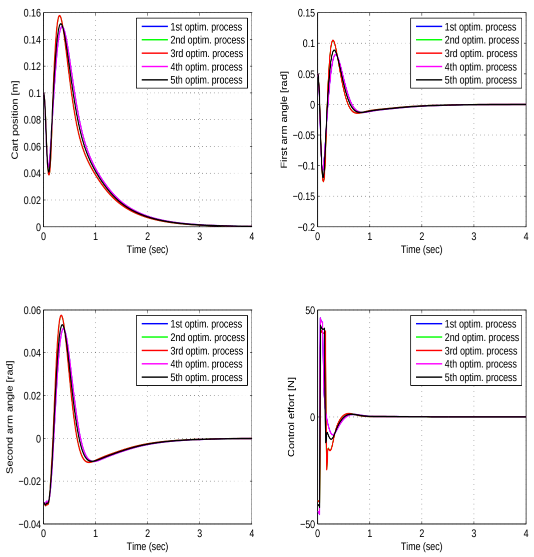

Figure 12: Repeated optimization process for unperturbed system at initial states $z = 0.1m$, $\theta = 0.05rad$, $\phi = -0.03rad$

6. Conclusion

This paper presents a methodological approach to design a state feedback sliding mode controller for class of unperturbed system and perturbed system with matched/mismatched uncertainties where the controller parameters are optimal tuned through the use of Genetic Algorithms. ADAMS/Matlab co-simulation environment is used in validating the proposed control scheme. For control design purposes, the nonlinear model is lin-

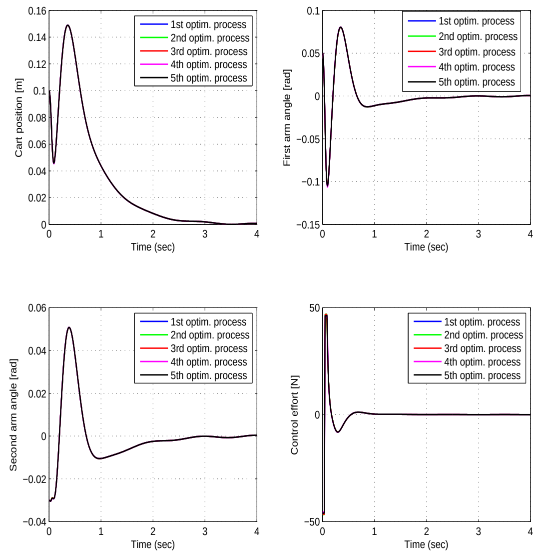

Figure 13: Repeated optimization process for perturbed system with matched uncertatinties at initial states $z = 0.1m$, $\theta = 0.05rad$, $\phi = -0.03rad$

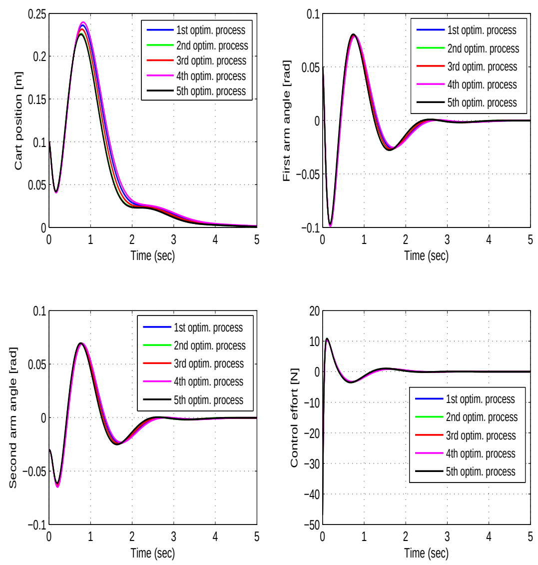

Figure 14: Repeated optimization process for perturbed system with mismatched uncertainties at initial states $z = 0.1m$, $\theta = 0.05rad$, $\phi = -0.03rad$

earized with parameters which vary within definite limits. Simulation results obtained from ADAMS/Matlab co-simulation affirm the robustness of the optimized sliding mode controller against payload variations and effectively removes chattering. The virtual environment that built by ADAMS assists relying on the results. The asymptotic stability is guaranteed with the existence of disturbances. As a future work, the proposed control technique will be applied to a real system for which sliding mode observer will be designed to estimate the states. A comparison between the proposed optimized state feedback sliding mode controller and other techniques will be investigated.

7. Acknowledgment

The first author is supported by a scholarship from the Mission Department, Ministry of Higher Education of the Government of Egypt which is gratefully acknowledged. Our sincere thanks to Egypt-Japan University of Science and Technology (E-JUST) for guidance and support.

The authors of the paper would like to thank Dr. Mohamed Fanni; Mechatronics and Robotics Dep. (E-JUST), at Egypt Japan University of Science and Technology for assistance and support in the work.

References

[1] K. Furuta, M. Yamakita, S. Kobayashi, Swing up control of inverted pendulum, in: Industrial Electronics, Control and Instrumentation, 1991. Proceedings. IECON '91., 1991 International Conference on, 1991, pp. 2193–2198 vol.3.

[2] K. J. Åström, K. Furuta, Swinging up a pendulum by energy control, Automatica 36 (2) (2000) 287–295.

[3] Y. Sang, Y. Fan, B. Liu, Double inverted pendulum control based on three-loop pid and improved bp neural network, in: Digital Manufacturing and Automation (ICDMA), 2011 Second International Conference on, IEEE, 2011, pp. 456–459.

[4] S. Zhang, S. Shao, R. An, S. Feng, Y. Du, The sliding mode variable structure control for double inverted pendulum system based on fuzzy reaching law, in: Advances in Electronic Engineering, Communication and Management Vol. 1, Springer, 2012, pp. 123–129.

[5] E. Vinodh Kumar, J. Jerome, Robust lqr controller design for stabilizing and trajectory tracking of inverted pendulum, Procedia Engineering 64 (2013) 169–178.

[6] K.-i. Nagasaka, H. Inoue, M. Inaba, Dynamic walking pattern generation for a humanoid robot based on optimal gradient method, in: Systems, Man, and Cybernetics, 1999. IEEE SMC'99 Conference Proceedings. 1999 IEEE International Conference on, Vol. 6, IEEE, 1999, pp. 908–913.

[7] B. Sheng, M. Huaqing, Z. Zhongjie, H. Quanyong, M. Huaxi, Z. Yanping, L. Shaojun, Walking control method of humanoid robot based on fsr sensors and inverted pendulum model, in: Advances in Autonomous Robotics, Springer, 2012, pp. 402–413.

[8] R. Watanabe, Motion control of nxtway (lego segway), Universidad de Waseda, Japón, disponible en http://web. mac. com/ryo watanabe/(Septiembre 2008).

[9] H. G. Nguyen, G. Kogut, R. Barua, A. Burmeister, N. Pezeshkian, D. Powell, N. Farrington, M. Wimmer, B. Cicchetto, C. Heng, et al., A segway rmp-based robotic transport system, in: Optics East, International Society for Optics and Photonics, 2004, pp. 244–255.

[10] S.-Y. Zhang, R. An, S.-M. Shao, D. Li, A new fuzzy controller for stabilization of double inverted pendulum system, in: Computer and Communication Technologies in Agriculture Engineering (CCTAE), 2010 International Conference On, Vol. 1, 2010, pp. 300–303. doi:10.1109/CCTAE.2010.5543607.

[11] O.Mehrez, A.Ramadan, , A. Aboismail, Stabilization of a loaded double inverted pendulum system, in: Egypt-Japan University of Science and Technology (E-JUST), 2011, pp. 44–53.

[12] C. Edwards, S. K. Spurgeon, Sliding mode control: theory and applications, Vol. 7, CRC Press, 1998.

[13] T. Fujinaka, Y. Kishida, M. Yoshioka, S. Omatu, Stabilization of double inverted pendulum with self-tuning neuro-pid, in: Neural Networks, 2000. IJCNN 2000, Proceedings of the IEEE-INNS-ENNS International Joint Conference on, Vol. 4, IEEE, 2000, pp. 345–348.

[14] V. Utkin, J. Guldner, M. Shijun, Sliding mode control in electromechanical systems, Vol. 34, CRC press, 1999.

[15] J. Ackermann, V. Utkin, Sliding mode control design based on ackermanns´ formula, Automatic Control, IEEE Transactions on 43 (2) (1998) 234–237.

[16] K.-K. Shyu, Y.-W. Tsai, C.-K. Lai, Sliding mode control for mismatched uncertain systems, Vol. 34, IET, 1998, pp. 2359–2360.

[17] A. Bogdanov, Optimal control of a double inverted pendulum on a cart, OGI School of Science and Engineering, OHSU.

[18] B. Draženović, The invariance conditions in variable structure systems, Automatica 5 (3) (1969) 287–295.

[19] Q. Ha, H. Trinh, H. Nguyen, H. Tuan, Dynamic output feedback sliding-mode control using pole placement and linear functional observers, Industrial Electronics, IEEE Transactions on 50 (5) (2003) 1030–1037.

[20] W. M. Bessa, M. S. Dutra, E. Kreuzer, Sliding mode control with adaptive fuzzy dead-zone compensation of an electro-hydraulic servo-system, Journal of Intelligent and Robotic Systems 58 (1) (2010) 3–16.

[21] H. H. Choi, Variable structure control of dynamical systems with mismatched norm-bounded uncertainties: an lmi approach, International Journal of Control 74 (13) (2001) 1324–1334.

[22] R. H. Takahashi, P. L. Peres, H 2 guaranteed cost-switching surface design for sliding modes with nonmatching disturbances, Automatic Control, IEEE Transactions on 44 (11) (1999) 2214–2218.

[23] C.-M. Kwan, Sliding mode control of linear systems with mismatched uncertainties, Automatica 31 (2) (1995) 303–307.

[24] J. Xiang, H. Su, J. Chu, W. Wei, Sliding surface matched condition in sliding mode control, Asian Journal of Control 9 (3) (2007) 345–351.

[25] A. Popov, Genetic algorithms for optimization, User Manual, Hamburg 2013.

[26] C.-C. Wong, S.-Y. Chang, Parameter selection in the sliding mode control design using genetic algorithms, Tamkang Journal of science and Engineering 1 (1998) 115–122.

[27] C. Edwards, S. Spurgeon, Sliding mode control: theory and applications, CRC Press, 1998.

[28] W. Perruquetti, J.-P. Barbot, Sliding mode control in engineering, CRC Press, 2002.

[29] J.-J. E. Slotine, W. Li, et al., Applied nonlinear control, Vol. 199, Prentice hall New Jersey, 1991.